

Spin cutoff factor and level density for ^{59}Ni from an analysis of compound nuclear reactions

A. V. Voinov¹,* N. Alanazi,[†] S. Akhtar,[‡] S. Dhakal,[‡] C. R. Brune, S. M. Grimes, T. N. Massey¹,
Z. Meisel, C. E. Parker,[§] and A. L. Richard¹

Department of Physics and Astronomy, Ohio University, Athens, Ohio 45701, USA



(Received 29 December 2022; accepted 28 June 2023; published 1 September 2023)

The spin cutoff parameter for ^{59}Ni has been studied from different types of experimental data including neutron angular distributions from the $^{56}\text{Fe}(\alpha, n)^{59}\text{Ni}$ reaction, spin of discrete levels, the level density from the proton evaporation spectrum of the $^{54}\text{Fe}(\alpha, p)^{59}\text{Ni}$ reaction and neutron resonance spacing. Experimental data points were compared with calculations using models widely used in literature. It was found that the available empirical models overestimate data points in the energy region below the neutron separation energy, while microscopic calculations which take into account pairing correlations within Hartree-Fock + Bardeen-Cooper-Schrieffer approach are consistent with data. It confirmed earlier findings that pairing correlations play an important role and need to be taken into account when the spin cutoff parameter is calculated below the neutron separation energy.

DOI: [10.1103/PhysRevC.108.034302](https://doi.org/10.1103/PhysRevC.108.034302)

I. INTRODUCTION

The nuclear level density plays an important role in modern nuclear reaction codes used for cross section calculations in the areas of basic nuclear physics, nuclear technology, astrophysics, and for the evaluation of nuclear data. Multiple models are available as input options in reaction codes such as EMPIRE [1] and TALYS [2]. Level density models are mostly based on the Fermi-gas model [3], the composite formula of Gilbert and Cameron [4], or microscopical calculations of Refs. [5,6]. However, there is still no well-established model which would work for all nuclei from different mass ranges. The nuclear level density is considered to be one of the least accurate input parameters in reaction codes, which results in sizable inaccuracy in cross section calculations. For the description of specific nuclear models, one can refer to descriptions of reaction code physics in Refs. [1,2].

In this work, we focus on the experimental study of the spin distribution of the nuclear level density $\rho(E, J)$, where E is the excitation energy and J is the nucleus spin. Phenomenological models use the following spin distribution function $g(E, J)$ to calculate the level density for the particular spin J :

$$\rho(E, J) = \rho(E) \cdot g(E, J), \quad (1)$$

where $\rho(E)$ is the total level density [3],

$$\rho(E) = \frac{\exp 2\sqrt{a(E - \Delta)}}{12\sqrt{2}\sigma(E)a^{1/4}(E - \Delta)^{5/4}}, \quad (2)$$

where a and Δ are the level density and back-shift parameters. An analytical expression for the $g(E, J)$ has been developed in Refs. [7] which is based on the model of non-interacting fermions with equidistant single particle levels and can be written in the Gaussian form as

$$g(E, J) = \frac{1}{\sigma(E)\sqrt{2\pi}} \cdot \exp\left[\frac{-J(J+1)}{2\sigma^2(E)}\right]. \quad (3)$$

The spin cutoff parameter $\sigma(E)$ determining the width of the distribution is expressed as

$$\sigma^2(E) = g_0 \langle m^2 \rangle t(E), \quad (4)$$

where $g_0 = 6a/\pi^2$ is the single particle state density, $\langle m^2 \rangle$ is an average of squares of single particle spin projections, and $t(E)$ is the temperature. The different final expressions used in literature for practical applications are based on different estimates of the $\langle m^2 \rangle$ value. Gilbert and Cameron [4] came up with the expression of $\langle m^2 \rangle = 0.146A^{2/3}$ which was deduced from the angular momentum analysis by Jensen and Luttinger [8]. Assuming that the $t(E) = \sqrt{(E - \Delta)/a}$, it gives us the following expression for the spin cutoff parameter:

$$\sigma_{GC}^2(E) = 0.088A^{2/3}\sqrt{a_{GC}(E - \Delta)}. \quad (5)$$

Bloch showed [9] that the average square of angular momentum projections can be related to the moment of inertia, I , with the expression of $\langle m^2 \rangle = I/(\hbar^2 g)$, so that

$$\sigma^2(E) = \frac{It(E)}{\hbar^2}. \quad (6)$$

If we assume a nucleus to be a rigid sphere with mass M and radius $R = r_0A^{1/3}$, the moment of inertia can be written as

*voinov@ohio.edu

[†]Present address: Physics and Astronomy Department, King Saud University, 12371 Riyadh, Saudi Arabia.

[‡]Present address: Montana Technological University, Butte, MT 59701, USA.

[§]Present address: Cyclotron Institute, Texas A&M University, College Station, Texas 77843, USA.

¹Present address: Lawrence Livermore National Laboratory, Livermore, CA 94550, USA.

$I = (2/5)MR^2$ and the spin cutoff is expressed as

$$\sigma_{RB}^2(E) = 0.0139A^{5/3}\sqrt{E/a_{RB}}. \quad (7)$$

This formula was suggested in Ref. [10] and used in the TALYS reaction code [2]. One should note that, in general, $a_{GC} \neq a_{RB}$, since these empirical parameters are found by fitting Eqs. (1), (2) to experimental data using different prescriptions for $\sigma(E)$.

While there is a general consensus (but still not proven experimentally for all nuclei) that the spin cutoff parameter values can be estimated with the rigid body formula (7) at the neutron separation energy and higher, it is still not clear how it behaves at lower excitation energies. The analysis of the spin distribution of discrete known levels [10] shows that the spin cutoff parameter is better described if we assume the half rigid body moment of inertia in Eq. (7). The paper of Ref. [11] studied the systematics of the spin distribution of discrete levels and established an empirical formula, which has a different excitation energy dependence compared to both Eqs. (5) and (7):

$$\sigma^2(E) = 0.389A^{0.675}(E - 0.5Pd)^{0.312}, \quad (8)$$

where the Pd is the deuteron separation energy. This formula was designed to reproduce the spin cutoff parameter for discrete low-lying levels, but it results in smaller parameter values at higher energies compared to Eq. (7).

In modern reaction computer codes, such as EMPIRE [1] and TALYS [2], in order to describe the spin distributions below the neutron separation energy, the linear interpolation is used between the spin cutoff parameter from discrete levels and that calculated with the rigid body formula (7) at higher excitation energies,

$$\sigma(E^*)^2 = \sigma_d^2 + \frac{E^* - E_d}{S_n - E_d}(\sigma_{RB}^2(S_n) - \sigma_d^2), \quad (9)$$

where σ_d^2 is calculated from known spins of discrete levels as follows [2]:

$$\sigma_d^2 = \frac{1}{3 \sum_{i=N_L}^{N_U} (2J_i + 1)} \sum_{i=N_L}^{N_U} J_i(J_i + 1)(2J_i + 1), \quad (10)$$

where J_i is the spin of discrete level i , N_L in the lower discrete level (usually this is a ground state), and N_U is the upper discrete level until which the level scheme is considered to be complete. E_d is defined as $E_d = \frac{1}{2}(E_L + E_U)$. Estimations of these parameters can be found in Ref. [10].

The spin cutoff parameter has been studied theoretically in a number of works. It has been shown from shell model calculations [12,13] that pairing effects reduce the spin cutoff parameter at low excitation energies compared to that calculated with the rigid body formula (7). Also, at excitation energies near the neutron separation threshold, quantum effects reflecting the population of individual orbits are not yet averaged out resulting in the spin cutoff parameter being below or above the rigid body values [14].

Experimental information about the spin cutoff parameter is scarce. In the region of discrete levels, it is calculated from known spins of levels. At higher excitation energies, the spin cutoff parameter was tested with the analysis of isomeric

cross section ratios [15] and with analysis of particle angular distributions from compound nuclear reactions [16–18] for nuclei in the 50–70 mass range. There is a strong indication from isomeric ratio studies that the spin cutoff parameter is reduced below the particle separation threshold compared to rigid body estimates. However, the reliability of the spin cutoff parameter values based on isomeric ratios data can be questionable since the isomeric ratio analysis requires full γ -cascade calculations which are affected not only by spin distributions but also by other parameters such as the nuclear level density and γ -strength functions which are also uncertain.

A technique based on an analysis of the angular distributions from compound reactions has been developed in the works of Refs. [19,20] using both classical and quantum mechanical approaches. In the classical approach, the angular distribution is determined by the following expression:

$$W(\Theta) = 1 + \frac{\bar{I}^2 \cdot \bar{l}^2}{12\sigma^4} P_2(\cos(\theta)), \quad (11)$$

where \bar{I}^2 and \bar{l}^2 are the average square of values of angular momenta of compound nucleus and outgoing particle, respectively, and the Legendre polynomial is approximated by $P_2(\cos(\Theta)) \simeq 2/3 \cdot \cos^2(\Theta)$. Equation (11) uses a number of approximations: it does not take into account spins of interacting particles, spin cutoff factors, and level densities for competing channels in a compound nuclear reaction. It is valid for small anisotropies $(\sigma(180^\circ)/\sigma(90^\circ)) - 1 \ll 1$. The more rigorous quantum mechanics approach of Ref. [20] is free from the above assumptions. It is based on the formula

$$W(\Theta) = \sum_{L(\text{even})} B_L(\epsilon_b) P_L(\cos(\Theta)), \quad (12)$$

where P are Legendre polynomials and B are coefficients taking into account spin and orbital momenta couplings with Clebsch-Gordan and Racah coefficients (see Ref. [20] for the full equation).

Results obtained from angular distributions in previous works appear to be inconclusive. Authors of Ref. [16] measured the spin cutoff parameter values from (α, n) reactions on nuclei from the 50–60 mass range. Because of large error bars, no conclusion was made on which empirical model is best to reproduce these values. However, there was an indication that the energy and mass dependence of the spin cutoff values are slower than predictions from models. Authors of Ref. [17] have estimated spin cutoff parameter values for ^{55}Fe and ^{59}Ni from (α, n) reactions. They found that values are smaller than rigid body estimates by a factor in the range of 0.3–0.6. However, no absolute values were presented. Authors of Ref. [18] studied the spin cutoff parameter also from the angular distribution of neutrons in the (α, n) reaction on nuclei from the mass range 50–120. The values were found to be smaller than the rigid body estimates by a factor of 0.8 on average, which is not consistent with the much smaller factor from Ref. [17] indicated above. Authors from Ref. [21] used (α, α) , (α, p) , and (p, α) reactions to study the spin cutoff parameter in the mass range near $A = 60$. Results were found to be consistent with rigid body estimates.

Results from previous works appear to be ambiguous regarding which estimation is valid. Specific values for rigid body estimates to which deduced spin cutoff values were compared to were not presented; they might have been different in different works. At this point it would be important to benchmark existing models with their specific parametrizations used in modern reaction computer codes such as TALYS [2] and EMPIRE [1] against experimental values to see if models can be constrained. This would be important for practical applications and for guiding development of theoretical models. Another concern which has not been discussed in previous works is that they did not take into account competition between reaction decay channels. The compound nucleus decay channels i which can be referred to as (T_i, E_i, L_i) , where T_i is a type of emitted particle i , E_i is a i -particle energy, and L_i is a particle orbital momentum. There must be an effect of cross influence between different channels in the (T, E, L) space, which has not been taken into account in previous works.

In this work, we focus on the ^{59}Ni nucleus. We studied neutron angular distributions from the $^{56}\text{Fe}(\alpha, n)^{59}\text{Ni}$ reaction experimentally. In addition, we reanalyzed some angular distribution data from (α, n) reactions in Refs. [16–18]. Compared to the analysis techniques used in previous works, this work implemented the following improvements: the assumption of the rigid body formula (7) on fixed energy dependence is not used anymore, the effect of the spin distribution in the competing (α, p) and (α, α') channels was taken into account and included in the uncertainty estimates. The quantum mechanics approach based on the work of Ref. [20] was implemented in the Hauser-Feshbach reaction code developed at Ohio University [22] and used for analysis of experimental angular distributions in this work.

II. EXPERIMENTS

Double differential cross sections of neutrons $d\sigma(E_n, \Theta)/(dE_n d\Theta)$ from the $^{56}\text{Fe}(\alpha, n)$ reaction with a 13 MeV α beam have been measured with the swinger facility of the tandem accelerator at the Edwards Accelerator Laboratory, Ohio University [23]. The beam swinger facility allows the beam rotation around the target position while a neutron detector is kept at the fixed location in the underground tunnel at the distance of 5 m from the target, for which a metal foil of about 0.5 mg/cm² thick enriched to 95% (^{56}Fe) was used. The liquid scintillator NE213 detector of 5×2 in. was used for neutron detection. The efficiency of the detector was determined from a separate run producing the standard neutron white spectrum in the range between 1–10 MeV from the $^{\text{nat}}\text{Al}(d, n)$ reaction [24]. Neutron energies were determined by time of flight technique with a pulsed beam of about 3 ns timing width. More details can be found in Ref. [25].

For the ^{56}Fe target, neutron spectra were measured at 20, 34, 45, 62, 76, 118, 135, and 146 degree angles in the laboratory frame. Spectra were corrected on detector efficiency, and converted to the center of mass frame. Angular distributions were extracted for the neutron energy intervals (E_1, E_2) : (2.5,3.4), (3.4,4.4), and (4.4,7.8) MeV. The first two intervals correspond to the population of the continuum region at

excitation energies higher than energies of known discrete levels of ^{59}Ni . The last interval corresponds to population of discrete levels which are known in the excitation energy range up to about 3.3 MeV. Data points for both neutron differential cross sections and angular distributions are shown in Fig. 1. The other experiment was conducted to study the proton evaporation spectrum from the $^6\text{Li} + ^{54}\text{Fe}$ reaction using the charged particle spectrometer at the Edwards Laboratory. First stage protons populate ^{59}Ni from the $^{54}\text{Fe}(^6\text{Li}, p)^{59}\text{Ni}$ reaction, so the level density was extracted from the proton spectrum according to the technique described in Ref. [26] and in our previous works [27]. Experimental details were presented in Ref. [28].

III. LEVEL DENSITY AND SPIN CUTOFF OF ^{59}Ni FROM PROTON EVAPORATION SPECTRUM

The proton double differential cross section measured at 142 degree angle and the extracted level density for ^{59}Ni are shown in Fig. 2. The experimental level density was compared with model calculations using the Fermi-gas formula (2), the spin distribution formula (3), and spin cutoff parameter equations (5), (7), (8). The parameters a and Δ were found from fitting Eq. (2) to the density of discrete levels and the neutron resonance spacing of $D_0 = 12.9$ keV at the neutron separation energy of $S_n = 9.0$ MeV taken from Ref. [29]. One can see from the comparison that the total level density values calculated with the Fermi-gas equation (2) at the neutron separation energy are sensitive to the spin cutoff parameter model used in calculation. The best agreement with the experiment is provided when the rigid body estimation (7) is used. The equations based on the Gilbert and Cameron (5) and Egidy (8) formulas result in underestimation of the total level densities at the neutron separation energy.

IV. SPIN CUTOFF FROM DISCRETE LEVELS

According to Ref. [10], the discrete level scheme of ^{59}Ni is considered to be complete up to around 3.6 MeV. The maximum excitation energy up to which spin assignments are uniquely known is 1.7 MeV. For the levels between 1.7 and 3.6 MeV, spin assignments are not well established, meaning that multiple spin values or no values are suggested. For the spin cutoff parameter estimation, all levels were used up to 3.1 MeV excitation energies. All of these levels have one or two alternative spin assignments from Ref. [30] with no levels having unassigned spins. All levels were grouped in bins and fitted with the spin distribution function (3). For levels with more than one spin assignment, spin values have been sampled randomly many times and for each realization the binning and fitting procedures were repeated. The final uncertainty for the spin cutoff parameter value includes the uncertainty due to a limited number of levels in each bin and the uncertainty related to unknown spins for some levels. The final number in the energy interval specified above was obtained to be $\sigma^2 = 6.1 \pm 0.9$. The spin distributions for both discrete levels and fit functions are shown in Fig. 3. Since levels are not distributed evenly over an excitation energy range, the average excitation energy for the estimated spin cutoff

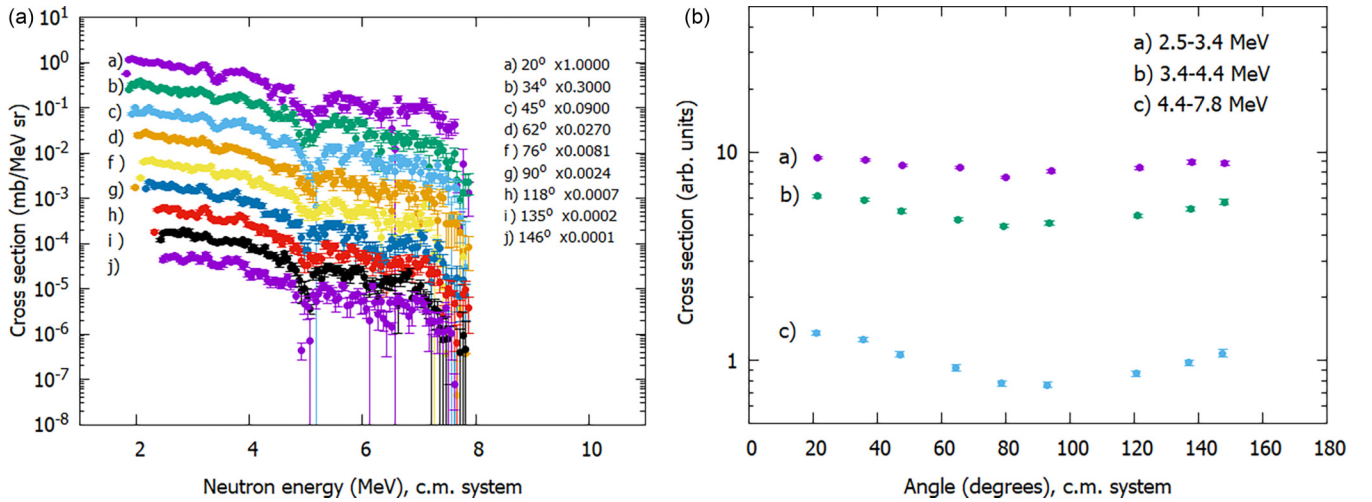


FIG. 1. Neutron spectra (left) and angular distributions (right) from the $^{56}\text{Fe}(\alpha, n)^{59}\text{Ni}$ reaction. Neutron energy intervals over which integration (13) was performed are (2.5,3.4), (3.4,4.4), and (4.4,7.8) MeV for the top, middle, and bottom distributions, respectively. All data points are in the center of mass system.

parameter value was calculated taking into account excitation energies of individual levels and found to be 2.2 ± 0.8 MeV.

V. SPIN CUTOFF FROM ANGULAR DISTRIBUTIONS

The Hauser-Feshbach computer code developed at the Edwards Accelerator Laboratory [31] was used to calculate an angular distribution function in the energy interval of outgoing neutrons between E_1 and E_2 :

$$W^{cal}(\Theta) = \int_{E_1}^{E_2} W^{cal}(\Theta, E_n) dE_n. \quad (13)$$

Calculations were based on the Douglas and MacDonald approach [20] which takes into account angular momenta and spins of incoming α and outgoing n , p , and α particles. This is important since all outgoing particles compete in both energy

and angular momentum spaces, and changing model parameters for one channel might affect the others.

To obtain spin cutoff parameter values and their uncertainties from experimental angular distributions, we employed the Monte Carlo technique in which the spin cutoff parameter excitation energy E function was parametrized as

$$\sigma^2(E) = \sigma_0^2 \left[\frac{E - E_0}{E_x - E_0} \right]^P. \quad (14)$$

Such a function comprises all known expressions for the spin cutoff parameter, at the same time allowing greater variability when parameters σ_0^2 , E_0 and P are varied. For each randomly generated set of parameters, the spin cutoff values were calculated and used as an input to the Hauser-Feshbach code to calculate neutron angular distributions. The level density function was parametrized with the constant temperature

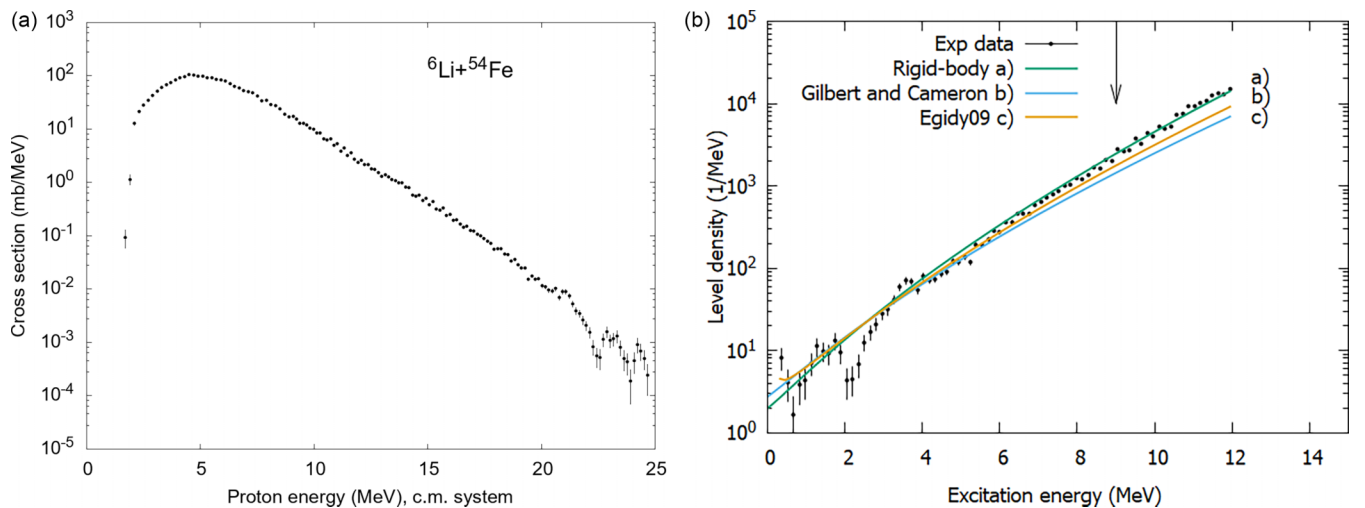


FIG. 2. Proton evaporation spectrum from $^{54}\text{Fe}(^6\text{Li}, Xp)$ reaction (left), the level density of the ^{59}Ni nucleus (right). Model calculations used the Fermi-gas formula (2) and spin cutoff parameter prescriptions of rigid-body (7), Gilbert and Cameron (5), and Egidy09 (8). The arrow in the right panel shows locations of the neutron separation energy of $S_n = 9$ MeV.

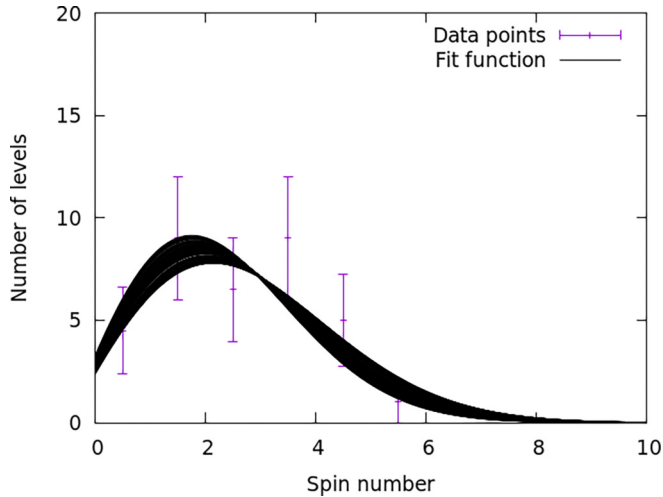


FIG. 3. Spin distribution obtained from analysis of discrete levels for ^{59}Ni . Uncertainties for the points include both statistical (from level counts) and ones related to uncertain spin assignments for some levels in the level scheme.

model

$$\rho(E) = 1/T \exp((E - E_0^{ct})/T), \quad (15)$$

where the temperature T and the energy shift E_0^{ct} were adjusted to reproduce the experimental level density for ^{59}Ni presented in Fig. 2. Parameters for ^{59}Co and ^{56}Fe populated with proton and α channels were taken from the Gilbert and Cameron [4] level density parameter table in Ref. [10]. Using the constant temperature approximation allows to decouple the level density from the spin cutoff parameter values in calculations. This allows studying the effect of the spin cutoff parameter independently of the level density $\rho(E)$ that would not be possible with the level density Fermi-gas formula (2) in which the total level density $\rho(E, \sigma)$ depends on the spin cutoff parameter. Parameters used are shown in Table I.

The angular distribution sampled for each parameter set was compared with an experimental one using the χ^2 function,

$$\chi^2 = \frac{1}{(N-1)} \sum_i^N \left(\frac{W_i^{\text{cal}} - W_i^{\text{exp}}}{\Delta W_i^{\text{exp}}} \right)^2, \quad (16)$$

where i is the index of a specific angle for which the experimental W^{exp} was measured and N is the number of angles. The special estimations were made for the values of the experimental error ΔW^{exp} . Because it is difficult to estimate systematic uncertainties, the following procedure to

TABLE I. Parameters and parameter intervals used in Eqs. (15) and (14), respectively.

| Reaction channel | T | E_0^{ct} | σ_0 | E_0 | P |
|---|-----|------------|------------|--------|---------|
| $^{56}\text{Fe}(\alpha, n)^{59}\text{Ni}$ | 1.4 | -2.07 | [2,12] | [-2,2] | [0,1.3] |
| $^{56}\text{Fe}(\alpha, p)^{59}\text{Co}$ | 1.3 | -1.9 | [2,12] | [-2,2] | [0,1.3] |
| $^{56}\text{Fe}(\alpha, \alpha')^{56}\text{Fe}$ | 1.4 | 1.4 | [2,12] | [-2,2] | [0,1.3] |

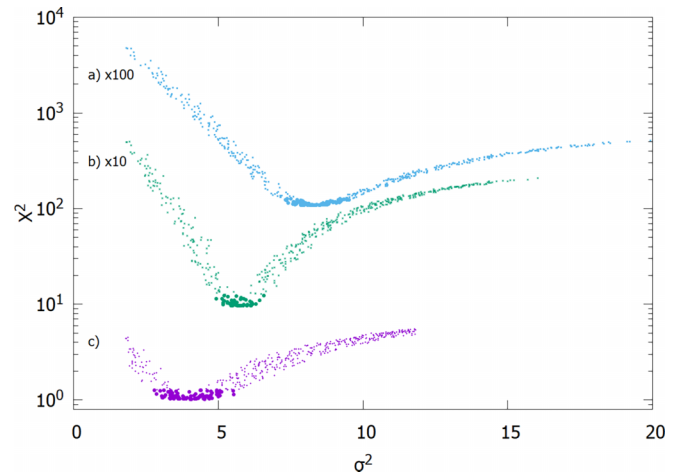


FIG. 4. The values of χ^2 (16) depending on σ^2 simulated with the formula (14). “a)” indicates points for (2.5,3.4) (multiplied by 100), “b)” for (3.4,4.4) (multiplied by 10), and “c)” for (4.4,7.8) neutron energy intervals. Points at the bottom of each valley indicate values which fall below the $\chi^2 = 1.3$ threshold.

estimate combined statistical and systematical uncertainties was adopted: the experimental angular distribution was fitted with a second order polynomial $P(\cos(\Theta))$ function and the value of ΔW^{exp} was calculated as

$$\Delta W^{\text{exp}} = \frac{1}{N} \sqrt{\sum_N (P^{\text{exp}}(\cos(\Theta)) - P(\cos(\Theta)))^2}. \quad (17)$$

This same value was used for all experimental points N , i.e., $\Delta W_{i=1\dots N}^{\text{exp}} = \Delta W^{\text{exp}}$. This uncertainty accounts for any uncertainty which contributes to a deviation of experimental points from a fitted polynomial curve. When these uncertainties are used, one can expect the χ^2 value (16) to be around one.

An approach based on Eqs. (16) and (14) allows estimating uncertainties of the spin cutoff parameter using the χ^2 distribution function (16). For $N = 8$ experimental angles, acceptance criteria for a “good” fit were found to be $\chi^2 < 1.3$ assuming 68% confidence interval. In simulation, parameters of Eq. (9) were randomly sampled in the intervals presented in Table I for all nuclei populated by neutrons, protons and α particles. Figure 4 presents χ^2 values (16) for neutron angular distributions in Fig. 1 depending on the values of the spin cutoff parameter σ^2 (14) simulated for the ^{59}Ni nucleus. One can see that for each neutron energy interval, the corresponding $\chi^2(\sigma^2)$ curve has a pronounced minimum. An additional scatter of the χ^2 values is due to the variation of spin cutoff values in proton and α channels, resulting in relative alteration of momentum space. The experimental spin cutoff parameter values derived from the simulation are shown in Fig. 5 in comparison with empirical models of Eqs. (5), (7), (8) as well as with values derived from microscopic calculations of Refs. [5,32]. Comparison shows that experimental points tend to fall below the rigid body estimate in the low energy range studied and might gradually approach it at higher energies. The formula of Eq. (8) appears to give a flatter excitation energy dependence, which is not supported by experimental points. Data support microscopic calculations taking into

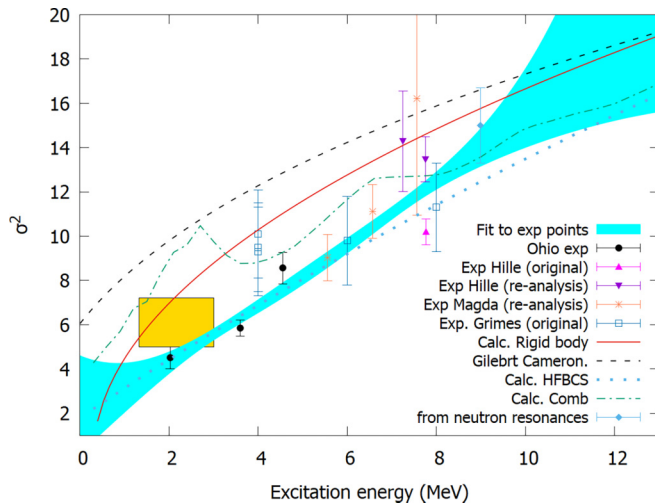


FIG. 5. Points are experimental values of the spin cutoff parameter derived from angular distributions, discrete level scheme, and neutron resonances. Lines are model calculations. The fit to all experimental data points and its uncertainty are shown by the shaded area. The shaded box at around 2 MeV shows the spin cutoff value derived from a discrete level scheme.

account pairing correlations within Hartree-Fock + Bardeen-Cooper-Schrieffer (HFBCS) approach of Ref. [32]. The same conclusion has been drawn in Ref. [33] where pairing correlations have been taken into account within the shell model Monte Carlo approach. Microscopic calculations based on the combinatorial approach of Ref. [5] which does not include pairing correlations, overestimate data points. Our data support the idea that the pairing correlations are responsible for the reduction of the moment of inertia and consequently the spin cutoff parameter at excitation energies below the neutron separation energy.

Reduction of the moment of inertia results in lower-spin values being favored in nuclear reactions. This might have important consequences for calculations of reaction cross sections and spectra of ejectiles, including γ rays. For example, a competition of high energy and low-energy γ transitions

populating levels below the neutron separation threshold from capture reactions is expected to be affected by the spin cutoff parameter excitation energy dependence. This might affect the energy distribution (spectrum) of γ transitions from capture reactions that might be important for consideration in different applications.

VI. SUMMARY

The spin cutoff parameter (4) determining the level density spin dependence (3) has been studied experimentally for the ^{59}Ni nucleus from the angular distribution of neutrons emitted from the $^{56}\text{Fe}(\alpha, n)$ reaction. Results were compared with similar results from the previous studies of [16–18] as well as with calculations based on the rigid body phenomenological formula (7) and with the microscopic calculations of [5,32]. Combining experimental results from all works and comparing them with calculations shows that, in the excitation energy range below about 8 MeV, experimental values of the spin cutoff parameter tend to be lower than calculations based on the rigid body model of Eq. (7), as well as calculations based on the combinatorial model of [5] which does not take into account pairing correlations. Microscopic calculations which take into account pairing correlations with the HFBCS model of Ref. [32] follow experimental points more closely. This effect is also consistent with conclusions of the shell model Monte Carlo model calculations with pairing effects [33] which show the reduction of the moment of inertia in the low-excitation energy region from the rigid body estimates.

Reduction of the spin cutoff parameter below the neutron separation energy appears to be an important effect which should be taken into account in practical calculations. However, the magnitude of the effect is yet to be studied across the chart of nuclides.

ACKNOWLEDGMENT

Authors acknowledge financial support from Department of Energy, Grants No. DE-NA0004073, No. DE-NA0003909, No. DE-NA0002905 and No. DE-FG02-88ER40387.

-
- [1] M. Herman, R. Capote, B. Carlson, P. Obložinský, M. Sin, A. Trkov, H. Wienke, and V. Zerkin, Empire: Nuclear reaction model code system for data evaluation, *Nucl. Data Sheets* **108**, 2655 (2007).
 - [2] A. J. Koning, S. Hilaire, and M. C. Duijvestijn, TALYS-1.2, in *Proceedings of the International Conference on Nuclear Data for Science and Technology, April 22–27, 2007, Nice, France*, edited by O. Bersillon, F. Gunsing, E. Bauge, R. Jacqmin, and S. Leray (EDP Sciences, 2008), p. 211.
 - [3] H. A. Bethe, An attempt to calculate the number of energy levels of a heavy nucleus, *Phys. Rev.* **50**, 332 (1936).
 - [4] A. Gilbert and A. G. W. Cameron, A composite nuclear-level density formula with shell corrections, *Can. J. Phys.* **43**, 1446 (1965).
 - [5] S. Goriely, S. Hilaire, and A. J. Koning, Improved microscopic nuclear level densities within the Hartree-Fock-Bogoliubov plus combinatorial method, *Phys. Rev. C* **78**, 064307 (2008).
 - [6] S. Hilaire, M. Girod, S. Goriely, and A. J. Koning, Temperature-dependent combinatorial level densities with the DIM Gogny force, *Phys. Rev. C* **86**, 064317 (2012).
 - [7] T. Ericson, The statistical model and nuclear level densities, *Adv. Phys.* **9**, 425 (1960).
 - [8] J. H. D. Jensen and J. M. Luttinger, Angular momentum distributions in the Thomas-Fermi model, *Phys. Rev.* **86**, 907 (1952).
 - [9] C. Bloch, Theory of nuclear level density, *Phys. Rev.* **93**, 1094 (1954).
 - [10] R. Capote, M. Herman, P. Obložinský, P. G. Young, S. Goriely, T. Belgya, A. V. Ignatyuk, A. J. Koning, S. Hilaire, V. A. Plujko,

- M. Avrigeanu, O. Bersillon, M. B. Chadwick, T. Fukahori, Z. Ge, Y. Han, S. Kailas, J. Kopecky, V. M. Maslov, G. Reffo *et al.*, Reference input parameter library (RIPL-3), *Nucl. Data Sheets* **110**, 3107 (2009).
- [11] T. von Egidy and D. Bucurescu, Experimental energy-dependent nuclear spin distributions, *Phys. Rev. C* **80**, 054310 (2009).
- [12] S. Goriely, A new nuclear level density formula including shell and pairing correction in the light of a microscopic model calculation, *Nucl. Phys. A* **605**, 28 (1996).
- [13] H. Nakada and Y. Alhassid, Total and Parity-Projected Level Densities of Iron-Region Nuclei in the Auxiliary Fields Monte Carlo Shell Model, *Phys. Rev. Lett.* **79**, 2939 (1997).
- [14] S. M. Grimes, A. V. Voinov, and T. N. Massey, Mass-number and excitation-energy dependence of the spin cutoff parameter, *Phys. Rev. C* **94**, 014308 (2016).
- [15] S. Sudár and S. Qaim, Mass number and excitation energy dependence of the $\theta_{\text{eff}}/\theta_{\text{rig}}$ parameter of the spin cut-off factor in the formation of an isomeric pair, *Nucl. Phys. A* **979**, 113 (2018).
- [16] S. M. Grimes, J. D. Anderson, J. W. McClure, B. A. Pohl, and C. Wong, Level density and spin cutoff parameters from continuum (p, n) and (α, n) spectra, *Phys. Rev. C* **10**, 2373 (1974).
- [17] M. T. Magda, A. Alevra, I. R. Lukas, D. Plostinaru, E. Trutia, and M. Molea, Statistical emission and nuclear level densities in (α, n) reactions, *Nucl. Phys. A* **140**, 23 (1970).
- [18] P. Hille, P. Speer, M. Hille, K. Rudolph, W. Assmann, and D. Evers, Spin dependence of the nuclear level density from angular distributions of (α, n) reactions, *Nucl. Phys. A* **232**, 157 (1974).
- [19] T. Ericson and V. Strutinski, Angular distribution in compound nucleus processes, *Nucl. Phys.* **8**, 284 (1958).
- [20] A. C. Douglas and N. Macdonald, Compound nucleus processes in medium mass nuclei, *Nucl. Phys.* **13**, 382 (1959).
- [21] C. C. Lu, L. C. Vaz, and J. R. Huizenga, Spin distribution of the nuclear level density, *Nucl. Phys. A* **197**, 321 (1972).
- [22] S. M. Grimes, A user's manual for the Hauser-Feshbach code HF2002, Internal Report No. INPP 04-03 (2004).
- [23] Z. Meisel, C. Brune, S. Grimes, D. Ingram, T. Massey, and A. Voinov, The Edwards Accelerator Laboratory at Ohio University, *Phys. Procedia* **90**, 448 (2017), Conference on the Application of Accelerators in Research and Industry, CAARI 2016, 30 October–4 November 2016, Fort Worth, TX, USA.
- [24] T. N. Massey, S. Al-Quraishi, C. E. Brient, J. F. Guillemette, S. M. Grimes, D. Jacobs, J. E. O'Donnell, J. Oldendick, and R. Wheeler, A measurement of the $^{27}\text{Al}(d, n)$ spectrum for use in neutron detector calibration, *Nucl. Sci. Eng.* **129**, 175 (1998).
- [25] N. Alanazi, Studying the fusion evaporation reaction (α, n) with ^{54}Fe , ^{56}Fe , ^{57}Fe , and ^{58}Fe , PhD thesis, Ohio University (2018).
- [26] H. Vonach, Extraction of Level Density Information from Non-resonance Reactions, in Proceedings of the IAEA Advisory Group Meeting on Basic and Applied Problems of Nuclear Level Densities, BNL Report No. BNL-NCS-51694, 1983, p. 247.
- [27] A. V. Voinov, T. Renstrøm, D. L. Bleuel, S. M. Grimes, M. Guttormsen, A. C. Larsen, S. N. Liddick, G. Perdikakis, A. Spyrou, S. Akhtar, N. Alanazi, K. Brandenburg, C. R. Brune, T. W. Danley, S. Dhakal, P. Gastis, R. Giri, T. N. Massey, Z. Meisel, S. Nikas *et al.*, Level densities of $^{74,76}\text{Ge}$ from compound nuclear reactions, *Phys. Rev. C* **99**, 054609 (2019).
- [28] A. V. Voinov, S. M. Grimes, C. R. Brune, T. Massey, and A. Schiller, Recent experimental results on level densities for compound reaction calculations, *EPJ Web Conf.* **21**, 05001 (2012).
- [29] S. F. Mughabghab, *Atlas of Neutron Resonances* (Elsevier, Amsterdam, 2006).
- [30] ENSDF database, <https://www.nndc.bnl.gov/ensdf/>, accessed 2022-07-22.
- [31] S. M. Grimes, A Hauser-Feshbach Code for Deformed Nuclei, Technical Report (2012).
- [32] P. Demetriou and S. Goriely, Microscopic nuclear level densities for practical applications, *Nucl. Phys. A* **695**, 95 (2001).
- [33] Y. Alhassid, M. Bonett-Matiz, S. Liu, A. Mukherjee, and H. Nakada, Recent advances in the microscopic calculations of level densities by the shell model Monte Carlo method, *EPJ Web Conf.* **69**, 00010 (2014).